ACS APPLIED NANO MATERIALS

www.acsanm.org

Letter

Five-Minute Magnetic Nanoparticle Spectroscopy-Based Bioassay for Ultrafast Detection of SARS-CoV-2 Spike Protein

Kai Wu,*,† Vinit Kumar Chugh,† Venkatramana D. Krishna,† Yongqiang Andrew Wang, Timothy D. Gordon, Maxim C.-J. Cheeran,* and Jian-Ping Wang*

Cite This: *ACS Appl. Nano Mater.* 2022, 5, 17503−17507

Read Online

ACCESS | Metrics & More | Article Recommendations

ABSTRACT: In this work, we report a 5-min magnetic particle spectroscopy (MPS)-based bioassay strategy. In our approach, surface-functionalized magnetic nanoparticles are incubated with target analytes at 37 °C with agitation for 3 min, and the MPS reading is then taken at the fifth minute. We prove the feasibility of 5 min ultrafast detection of SARS-CoV-2 spike protein with a detection limit below 5 nM (0.2 pmol). Our proposed 5-min bioassay strategy may be applied to reduce the assay time for other liquid-phase, volumetric biosensors such as NMR, quantum dots, fluorescent biosensors, etc.

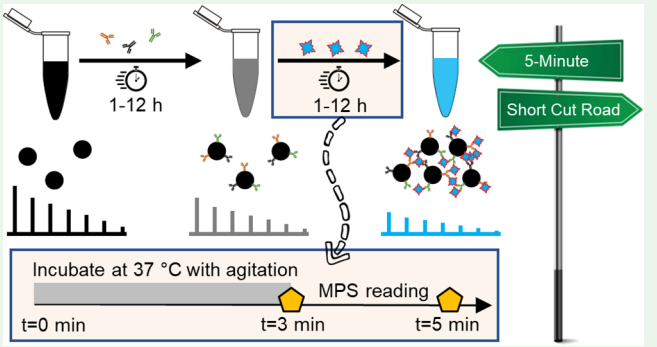

KEYWORDS: *magnetic particle spectroscopy, magnetic nanoparticle, SARS-CoV-2, bioassay, spike protein, volumetric biosensor*

With the ongoing coronavirus disease 2019 (COVID-19) pandemic, there is an urgent need for rapid, convenient, and widely deployable diagnosis tools for the surveillance of severe acute respiratory syndrome-coronavirus-2 (SARS-CoV-2), in a joint effort to mitigate its spread within and across communities. A rapid and sensitive method for early detection of SARS-CoV-2 is critical for controlling the spread of COVID-19 by proper containment procedures as well as for reducing morbidity and mortality by facilitating early treatment. Currently, the fastest on-site detection techniques such as lateral flow assays and ID Now can detect COVID-19 in 15−30 min. For most on-site diagnosis platforms, the bioassay time varies from 1 to 12 h. As a result, the long turnaround time has severely hindered COVID-19 surveillance and impeded pandemic control measures. Magnetic particle spectroscopy (MPS) is an emerging bioassay platform that has been used extensively in the areas of oncology, food safety, bacteria, and virus detection. Although it has been reported that portable MPS devices with low assay costs and easy-to-use features can be used for potential field testing, these MPS systems share the same drawback with most point-of-care (POC) diagnosis techniques, which is the long bioassay time.

MPS was originally derived from magnetic particle imaging in 2006 and has now developed into a mature bioassay technique.[1−4] To date, two types of MPS bioassay platforms have been reported, namely, surface- and volumetric-based MPS bioassays. Both platforms rely on monitoring of the dynamic magnetic responses of magnetic nanoparticles (MNPs), albeit using different mechanisms. Surface-based MPS bioassay platforms are usually combined with lateral flow strips or nonmagnetic porous filters that are surface-functionalized to specifically capture target biochemical analytes and MNPs. This surface-based MPS bioassay strategy has been reported for the detection of SARS-CoV-2,[5] plant viruses,[6] toxins,[7−9] and drugs.[10] On the other hand, volumetric-based MPS bioassay quantifies biochemical analytes through a change of the dynamic magnetic responses of freely rotating MNPs before and after the specific binding events. By using specially designed, surface-functionalized MNPs, the presence of target biochemical analytes causes different degrees of MNP clustering (Scheme 1), which impedes the Brownian relaxation of MNPs under an alternating-current magnetic field. Thus, weaker dynamic magnetic responses and lower harmonic amplitudes (i.e., MPS spectra) are observed.[1] This volumetric-based MPS bioassay strategy has been reported for the detection of SARS-CoV-2,[11,12] H1N1 virus,[13] thrombin and DNA aptamers,[14] and hormones and cytokines.[15]

Compared to surface-based MPS bioassay, this homogeneous and volumetric MPS bioassay strategy can be easily

Received: December 6, 2022
Accepted: December 9, 2022
Published: December 13, 2022

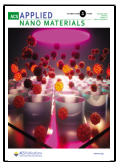

https://doi.org/10.1021/acsanm.2c05237
ACS Appl. Nano Mater. 2022, 5, 17503−17507

Scheme 1. Traditional MPS Bioassays as Well as Other Volumetric-Based Assay Platforms Require 1−12 h of Incubation Time as Shown in Step ii[a]

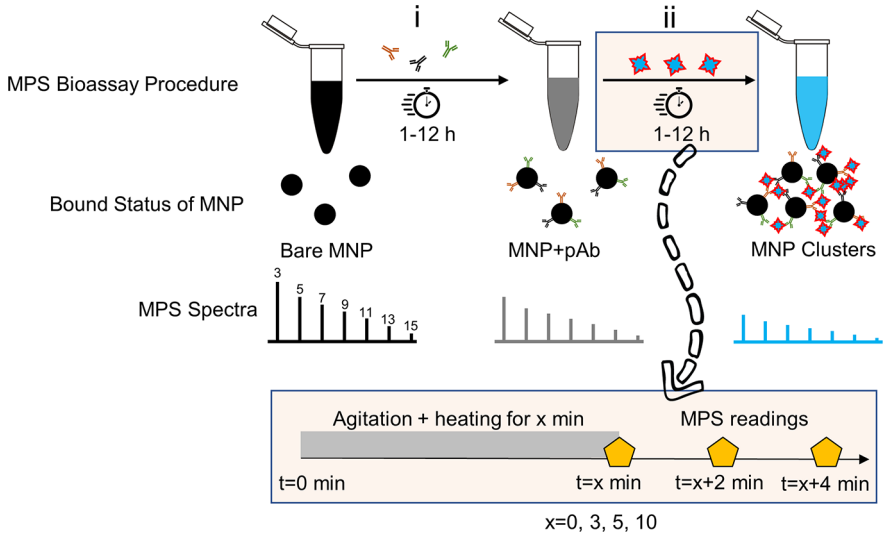

[a]Herein, incubation conditions (agitation and heating) are applied during the incubation step to result in ultrafast MPS bioassay (top row). (i) MNP surface functionalization with polyclonal antibodies. (ii) Surface-functionalized MNPs incubating with target analytes.

Table 1. Incubation Condition Experimental Design

temperature	without agitation			with agitation		
25 °C (no heating)	0 min, control group, no actions taken (group 1)			3 min (group 2)	5 min (group 3)	10 min (group 4)
32 °C (heating)	3 min (group 5)	5 min (group 6)	10 min (group 7)	3 min (group 8)	5 min (group 9)	10 min (group 10)
37 °C (heating)	3 min (group 11)	5 min (group 12)	10 min (group 13)	3 min (group 14)	5 min (group 15)	10 min (group 16)
42 °C (heating)	3 min (group 17)	5 min (group 18)	10 min (group 19)	3 min (group 20)	5 min (group 21)	10 min (group 22)

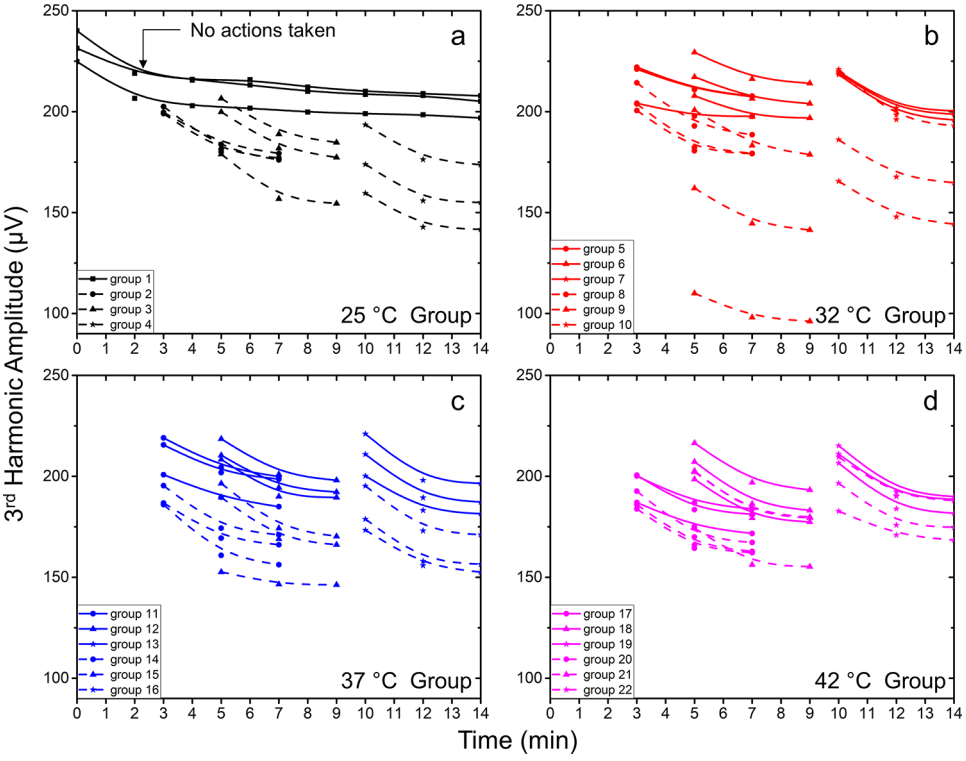

Figure 1. Summary of the MPS readings recorded from samples that have undergone different incubation conditions, categorized by incubation temperatures: (a) 25 °C; (b) 32 °C; (c) 37 °C; (d) 42 °C. The first data point of each curve indicates the incubation time. Solid and dashed lines indicate without and with agitation, respectively. The bottom outlier in group 9 in part b is caused by air bubbles introduced into the vial during the incubation step. This outlier is removed before further data analysis.

https://doi.org/10.1021/acsanm.2c05237
ACS Appl. Nano Mater. 2022, 5, 17503−17507

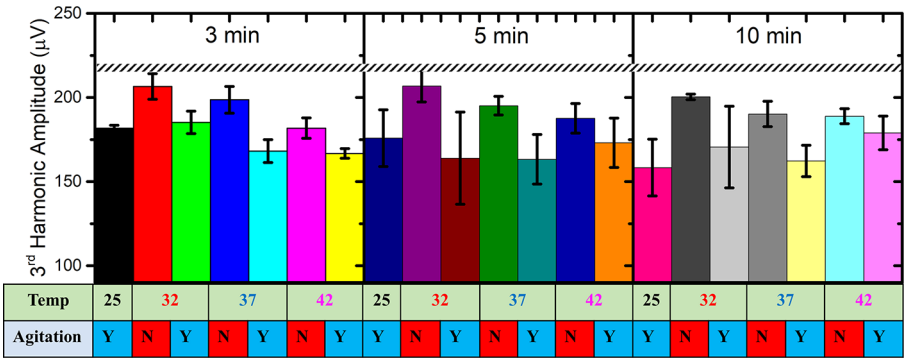

Figure 2. Histograms of the third harmonic recorded at $t = x + 2$ min. The horizontal line at $y = 220$ μV represents the averaged third-harmonic amplitude collected from control group 1, where no actions are taken during the incubation step. Signals are averaged over three independent bioassays. Error bars represent standard errors. "N" and "Y" indicate without and with agitation.

adapted into a one-step, wash-free testing kit for on-site applications, due to its ease of use. The end users simply mix the surface-functionalized MNPs with the liquid sample and take MPS readings. However, the bioassay step usually takes 1−12 h until the specific binding stabilizes at equilibrium (see step ii in Scheme 1). This delay is a major obstacle to the transfer of volumetric MPS bioassays from laboratory to field testing.

Herein, we explored the possibility of reducing the bioassay time by heating and agitating samples during the bioassay step (i.e., step ii in Scheme 1). The thermal energy and vibrational kinetic energy (caused by agitation) could increase the frequency of successful collisions between capture probes (i.e., pAb in this work) and target analytes (i.e., SARS-CoV-2 spike protein in this work), thus allowing for faster specific binding and shorter diagnosis turnaround time. As shown in Table 1, we varied three factors in the incubation condition experiment: time, temperature, and agitation. The incubation time was set at 0 min (control group, no actions taken), 3, 5, and 10 min. The incubation temperature influences the antigen−antibody affinity as well as the reaction rate. The temperature was set at 25 °C (room temperature, no heating), 32, 37, and 42 °C, respectively, in an incubator. These temperatures were randomly selected to range from room temperature (25 °C) to pathophysiological temperature (42 °C). Agitation was applied by placing the tubes in a Vortex Genie 2 mixer (Fisher Scientific model G-560) set at shaker speed of 2. Three independent bioassays were carried out under each incubation condition. A total of 22 experimental groups were designed, where 66 samples were prepared for MPS testing.

The IPG30 MNPs (30 nm iron oxide nanoparticles coated with protein G, 34 nM) were first surface-functionalized with anti-SARS-CoV-2 spike polyclonal antibodies (rabbit pAb, catalog no. 40592-T62, Sino Biological Inc.), as shown in step i in Scheme 1. The MNP-to-pAb ratio was precisely controlled at 1:3, where theoretically each MNP was functionalized with three pAb. This ratio was optimized based on our previous work.[11] Then, 40 μL of pAb-functionalized MNP complexes (denoted as MNP + pAb in this work) was mixed with 40 μL of 10 nM SARS-CoV-2 spike protein (catalog no. 40592-V08H, Sino Biological Inc.) in phosphate-buffered saline (PBS) without calcium and magnesium, pH 7.4 (Genesee Scientific, USA), and incubated under different conditions for x minutes (x = 0, 3, 5, and 10). Subsequently, the sample was transferred to the MPS platform at an ambient temperature of 10 °C, and three consecutive MPS readings were taken at $t = x$ min, $x + 2$ min, and $x + 4$ min, respectively. The MPS platform consisted of a benchtop system utilizing a pair of magnetic field generation coils, one pick-up coil, a data acquisition card by NI, and a LabVIEW setup, as has been detailed in our previous work.[16] There are two purposes of taking MPS readings in an ambient temperature of 10 °C: (1) to stop the antibody−antigen binding events after x minutes of incubation; (2) the MPS signal is also affected by the temperature;[17] thus, after incubation under different temperatures, samples should be brought back to the same ambient temperature for MPS readings.

Figure 1 summarizes the three consecutive MPS readings from samples subjected to different incubation conditions, categorized by the incubation temperatures. Only the third-harmonic amplitudes from MPS readings are plotted and compared because higher harmonics such as the fifth, seventh, ninth, etc., show similar trends. For the control group 1 (solid lines in Figure 1a), where no actions are taken during the incubation step, the third-harmonic amplitude drops slowly over the 14 min MPS reading window. Because each target SARS-CoV-2 spike protein molecule hosts multiple distinct epitopes that provide specific binding sites for pAb. The presence of target analytes (spike protein) causes the cross-linking of MNPs and hinders the Brownian motion of MNPs as well as weakens the dynamic magnetic response (Scheme 1). Thus, this drop in the real-time harmonic amplitude indicates that antibody−antigen specific binding is taking place, but at a slow rate.

The lower harmonic amplitudes indicate higher degrees of MNP clustering with more binding events. The dashed lines (with agitation) show lower amplitudes than the solid lines for all temperature groups in Figure 1. Thus, it was concluded that, for the same incubation time and temperature, agitation can effectively accelerate antibody−antigen binding. Because all of the samples are tested at an ambient temperature of 10 °C, the sudden temperature drop causes a lower harmonic amplitude at $t = x + 2$ min, and it becomes stable at $t = x + 4$ min (Figure 1). Thus, in order to compare the heating effect in the incubation step, the first MPS readings (taken at $t = x$ min) should not be used. Herein, we systematically compared the MPS harmonic signals from all experimental groups in Figure 2. The third-harmonic amplitudes are extracted from the second MPS readings (i.e., taken at $t = x + 2$ min) and averaged over three independent bioassays. For all of the experimental groups, the harmonic amplitudes are lower than

https://doi.org/10.1021/acsanm.2c05237
ACS Appl. Nano Mater. 2022, 5, 17503−17507

the harmonic amplitude of control group 1 (where no actions are taken during the incubation step, marked as a horizontal line in Figure 2). Without agitation, all experimental samples under heating conditions (i.e., at 32, 37, and 42 °C) show lower harmonic amplitudes than control group 1. In addition, for the without agitation scenarios, we noted that, for the same incubation time, a higher incubation temperature favors faster antibody−antigen binding, so lower harmonic amplitudes are observed. A longer incubation time favors more antibody−antigen binding events at the same temperature when agitation is absent. When agitation is applied, heating can still accelerate antibody−antigen binding. However, if the incubation time is long (such as 5 or 10 min), the effect of heating becomes less important. For example, by incubating for 3 min with agitation, a higher incubation temperature favors faster binding (as observed by the lower harmonic amplitudes). However, by incubating for 5 or 10 min with agitation, the harmonic amplitude of the heated sample is not significantly different from that of the unheated samples (i.e., at 25 °C).

From the above discussion, it was concluded that the best incubation conditions to effectively accelerate the binding process is incubation of the sample at 37 °C with agitation for 3 min. Note that reducing the incubation time is our priority; thus, although incubations at 32 °C with agitation for 5 min or at 37 °C with agitation for 5 min or at 25 °C with agitation for 10 min show similar results, they are less favorable than incubation at 37 °C with agitation for 3 min.

On the basis of the above incubation experiment, we propose an ultrafast MPS bioassay strategy: (1) incubate samples at 37 °C with agitation for 3 min, (2) transfer the mixture to an ambient temperature of 10 °C, and (3) collect the second MPS data point (at $t = x + 3 = 5$ min). As a proof of concept, we further tested this 5-min MPS bioassay strategy on different concentrations of a SARS-CoV-2 spike protein, from 1000 to 0.5 nM. This experiment was conducted on a two-stage lock-in MPS system with an additional voltage gain of around 32 dB for improved bioassay sensitivity. The concentration−response curve is plotted in Figure 3. Five independent bioassays were carried out at each concentration. The third-harmonic amplitude saturates at 500−1000 nM (upper concentration limit) and 0.5−1 nM (lower concentration limit), with a nearly linear response curve between these two limits. As schematically shown in Figure 3, with higher concentrations of SARS-CoV-2 spike protein added, the degree of MNP clustering increases, and the dynamic magnetic response of MNPs becomes weaker; thus, lower harmonic amplitudes are observed.

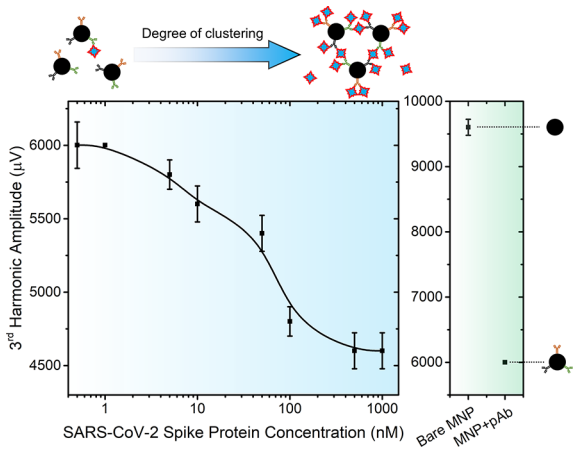

Figure 3. Concentration−response curve of a SARS-CoV-2 spike protein tested by a 5-min MPS bioassay strategy developed in this work. Five independent bioassays were carried out at each concentration. Error bars represent standard errors.

The averaged third-harmonic signals from active experimental samples range from 4500 to 6000 μV for samples with SARS-CoV-2 spike protein concentrations varying from 1000 to 0.5 nM. For comparison, the third-harmonic amplitudes of bare MNPs (IPG30 without pAb functionalization) and pAb-functionalized MNPs (denoted as MNP + pAb) are 9600 and 6000 μV, respectively. Because the pAb conjugated on MNPs impedes the Brownian relaxations, weaker MPS signals are expected from the MNP + pAb samples. The detection limit of this 5-min MPS bioassay for a SARS-CoV-2 spike protein is somewhere between 1 and 5 nM.

In summary, on the basis of this work, we propose the application of higher temperatures (37 °C) and agitation conditions during the MPS bioassay incubation step to accelerate the antibody−antigen specific binding. The thermal energy (heating) and vibrational kinetic energy (agitation) increase the frequency of successful collisions between SARS-CoV-2 spike pAbs (from the MNP surface) and the spike protein molecules, allowing for the faster establishment of specific binding equilibrium and shorter diagnosis turnaround time. Shortening of the assay time for MPS-based bioassay allows for the practical deployment of a POC system as well as increases the disease screening capacity. This is the first time that the impact of agitation and heating along with a combination of the two have been studied for MPS-based bioassay implementations. Our results show that the 5-min volumetric MPS bioassay strategy described here could be an effective way to cut the current COVID-19 diagnosis time from 1 h to 5 min. This quick turnaround in diagnosis will greatly advance surveillance and control strategies for diseases especially for future pandemics. Although this proof-of-concept was demonstrated on the volumetric MPS bioassay platform, it can also be applied to other volumetric biosensors such as NMR biosensors,[18,19] ferromagnetic resonance biosensors,[20] some types of fluorescent biosensors,[21] gold-nanoparticle-based colorimetric assays,[22] etc.

AUTHOR INFORMATION

Corresponding Authors

Kai Wu − *Department of Electrical and Computer Engineering, University of Minnesota, Minneapolis, Minnesota 55455, United States;* Present Address: Department of Electrical and Computer Engineering, Texas Tech University, Lubbock, TX 79409; Email: wuxx0803@umn.edu

Maxim C.-J. Cheeran − *Department of Veterinary Population Medicine, University of Minnesota, St. Paul, Minnesota 55108, United States*; Email: cheeran@umn.edu

Jian-Ping Wang − *Department of Electrical and Computer Engineering, University of Minnesota, Minneapolis, Minnesota 55455, United States*; Email: jpwang@umn.edu

Authors

Vinit Kumar Chugh − *Department of Electrical and Computer Engineering, University of Minnesota, Minneapolis, Minnesota 55455, United States*

https://doi.org/10.1021/acsanm.2c05237
ACS Appl. Nano Mater. 2022, 5, 17503−17507

Venkatramana D. Krishna − *Department of Veterinary Population Medicine, University of Minnesota, St. Paul, Minnesota 55108, United States*
Yongqiang Andrew Wang − *Ocean Nano Tech LLC, San Diego, California 92126, United States*
Timothy D. Gordon − *Aerosol Devices Inc., Fort Collins, Colorado 80524, United States*

Complete contact information is available at: https://pubs.acs.org/10.1021/acsanm.2c05237

Author Contributions

†K.W., V.K.C., and V.D.K. have contributed equally to this work.

Notes

The authors declare no competing financial interest.

■ ACKNOWLEDGMENTS

This study was financially supported by the Institute of Engineering in Medicine, the Robert F. Hartmann Endowed Chair professorship, the University of Minnesota Medical School, and the University of Minnesota Physicians and Fairview Health Services through a COVID-19 Rapid Response Grant. This study was also financially supported by the U.S. Department of Agriculture, National Institute of Food and Agriculture, under Award 2020-67021-31956. Research reported in this publication was supported by the National Institute of Dental & Craniofacial Research of the National Institutes of Health under Award R42DE030832. The content is solely the responsibility of the authors and does not necessarily represent the official views of the National Institutes of Health. Portions of this work were conducted in the Minnesota Nano Center, which is supported by the National Science Foundation through the National Nano Coordinated Infrastructure Network under Award ECCS-1542202.

■ REFERENCES

(1) Wu, K.; Su, D.; Saha, R.; Liu, J.; Chugh, V. K.; Wang, J.-P. Magnetic Particle Spectroscopy: A Short Review of Applications Using Magnetic Nanoparticles. *ACS Appl. Nano Mater.* **2020**, *3* (6), 4972−4989.
(2) Wu, K.; Su, D.; Saha, R.; Wong, D.; Wang, J.-P. Magnetic Particle Spectroscopy-Based Bioassays: Methods, Applications, Advances, and Future Opportunities. *J. Phys. Appl. Phys.* **2019**, *52*, 173001.
(3) Nikitin, P. I.; Vetoshko, P. M.; Ksenevich, T. I. New Type of Biosensor Based on Magnetic Nanoparticle Detection. *J. Magn. Magn. Mater.* **2007**, *311*, 445−449.
(4) Krause, H.-J.; Wolters, N.; Zhang, Y.; Offenhäusser, A.; Miethe, P.; Meyer, M. H.; Hartmann, M.; Keusgen, M. Magnetic Particle Detection by Frequency Mixing for Immunoassay Applications. *J. Magn. Magn. Mater.* **2007**, *311*, 436−444.
(5) Pietschmann, J.; Voepel, N.; Voß, L.; Rasche, S.; Schubert, M.; Kleines, M.; Krause, H.-J.; Shaw, T. M.; Spiegel, H.; Schroeper, F. Development of Fast and Portable Frequency Magnetic Mixing-Based Serological SARS-CoV-2-Specific Antibody Detection Assay. *Front. Microbiol.* **2021**, *12*, 841.
(6) Rettcher, S.; Jungk, F.; Kühn, C.; Krause, H.-J.; Nölke, G.; Commandeur, U.; Fischer, R.; Schillberg, S.; Schröper, F. Simple and Portable Magnetic Immunoassay for Rapid Detection and Sensitive Quantification of Plant Viruses. *Appl. Environ. Microbiol.* **2015**, *81* (9), 3039−3048.
(7) Pietschmann, J.; Spiegel, H.; Krause, H.-J.; Schillberg, S.; Schröper, F. Sensitive Aflatoxin B1 Detection Using Nanoparticle-Based Competitive Magnetic Immunodetection. *Toxins* **2020**, *12* (5), 337.
(8) Orlov, A. V.; Znoyko, S. L.; Cherkasov, V. R.; Nikitin, M. P.; Nikitin, P. I. Multiplex Biosensing Based on Highly Sensitive Magnetic Nanolabel Quantification: Rapid Detection of Botulinum Neurotoxins A, B, and E in Liquids. *Anal. Chem.* **2016**, *88* (21), 10419−10426.
(9) Bragina, V. A.; Znoyko, S. L.; Orlov, A. V.; Pushkarev, A. V.; Nikitin, M. P.; Nikitin, P. I. Analytical Platform with Selectable Assay Parameters Based on Three Functions of Magnetic Nanoparticles: Demonstration of Highly Sensitive Rapid Quantitation of Staphylococcal Enterotoxin B in Food. *Anal. Chem.* **2019**, *91* (15), 9852−9857.
(10) Guteneva, N. V.; Znoyko, S. L.; Orlov, A. V.; Nikitin, M. P.; Nikitin, P. I. Rapid Lateral Flow Assays Based on the Quantification of Magnetic Nanoparticle Labels for Multiplexed Immunodetection of Small Molecules: Application to the Determination of Drugs of Abuse. *Microchim. Acta* **2019**, *186* (9), 621.
(11) Wu, K.; Chugh, V. K.; D. Krishna, V.; di Girolamo, A.; Wang, Y. A.; Saha, R.; Liang, S.; Cheeran, M. C.; Wang, J.-P. One-Step, Wash-Free, Nanoparticle Clustering-Based Magnetic Particle Spectroscopy Bioassay Method for Detection of SARS-CoV-2 Spike and Nucleocapsid Proteins in the Liquid Phase. *ACS Appl. Mater. Interfaces* **2021**, *13* (37), 44136−44146.
(12) Zhong, J.; Rösch, E. L.; Viereck, T.; Schilling, M.; Ludwig, F. Toward Rapid and Sensitive Detection of SARS-CoV-2 with Functionalized Magnetic Nanoparticles. *ACS Sens.* **2021**, *6* (3), 976−984.
(13) Wu, K.; Liu, J.; Saha, R.; Su, D.; Krishna, V. D.; Cheeran, M. C.-J.; Wang, J.-P. Magnetic Particle Spectroscopy for Detection of Influenza A Virus Subtype H1N1. *ACS Appl. Mater. Interfaces* **2020**, *12* (12), 13686−13697.
(14) Zhang, X.; Reeves, D. B.; Perreard, I. M.; Kett, W. C.; Griswold, K. E.; Gimi, B.; Weaver, J. B. Molecular Sensing with Magnetic Nanoparticles Using Magnetic Spectroscopy of Nanoparticle Brownian Motion. *Biosens. Bioelectron.* **2013**, *50*, 441−446.
(15) Gordon-Wylie, S. W.; Ness, D. B.; Shi, Y.; Mirza, S. K.; Paulsen, K. D.; Weaver, J. B. Measuring Protein Biomarker Concentrations Using Antibody Tagged Magnetic Nanoparticles. *Biomed. Phys. Eng. Express* **2020**, *6* (6), 065025.
(16) Wu, K.; Liu, J.; Su, D.; Saha, R.; Wang, J.-P. Magnetic Nanoparticle Relaxation Dynamics-Based Magnetic Particle Spectroscopy for Rapid and Wash-Free Molecular Sensing. *ACS Appl. Mater. Interfaces* **2019**, *11* (26), 22979−22986.
(17) Draack, S.; Viereck, T.; Nording, F.; Janssen, K.-J.; Schilling, M.; Ludwig, F. Determination of Dominating Relaxation Mechanisms from Temperature-Dependent Magnetic Particle Spectroscopy Measurements. *J. Magn. Magn. Mater.* **2019**, *474*, 570−573.
(18) Luo, Y.; Alocilja, E. C. Portable Nuclear Magnetic Resonance Biosensor and Assay for a Highly Sensitive and Rapid Detection of Foodborne Bacteria in Complex Matrices. *J. Biol. Eng.* **2017**, *11* (1), 14.
(19) Lee, H.; Sun, E.; Ham, D.; Weissleder, R. Chip-NMR Biosensor for Detection and Molecular Analysis of Cells. *Nat. Med.* **2008**, *14* (8), 869.
(20) Tian, B.; Liao, X.; Svedlindh, P.; Strömberg, M.; Wetterskog, E. Ferromagnetic Resonance Biosensor for Homogeneous and Volumetric Detection of DNA. *ACS Sens.* **2018**, *3* (6), 1093−1101.
(21) Cheong, J.; Yu, H.; Lee, C. Y.; Lee, J.; Choi, H.-J.; Lee, J.-H.; Lee, H.; Cheon, J. Fast Detection of SARS-CoV-2 RNA via the Integration of Plasmonic Thermocycling and Fluorescence Detection in a Portable Device. *Nat. Biomed. Eng.* **2020**, *4* (12), 1159−1167.
(22) Moitra, P.; Alafeef, M.; Dighe, K.; Frieman, M. B.; Pan, D. Selective Naked-Eye Detection of SARS-CoV-2 Mediated by N Gene Targeted Antisense Oligonucleotide Capped Plasmonic Nanoparticles. *ACS Nano* **2020**, *14* (6), 7617−7627.